



Full Length Article

Effect of celecoxib and cisplatin combination on apoptosis and cell proliferation in a mouse model of chemically-induced colonic aberrant crypt foci

Soha S. Essawy^a, Shymaa E. Bilasy^b, Hala M.F. Mohammad^{a,*}, Aly A.M. Shaalan^c^a Department of Pharmacology, Faculty of Medicine, Suez Canal University, Ismailia, Egypt^b Department of Biochemistry, Faculty of Pharmacy, Suez Canal University, Ismailia, Egypt^c Department of Histology and Cell Biology, Faculty of Medicine, Suez Canal University, Ismailia, Egypt

ARTICLE INFO

Article history:

Received 25 March 2017

Received in revised form 22 June 2017

Accepted 17 July 2017

Available online 27 July 2017

Keywords:

BAX

Bcl2

Caspase-3

Celecoxib

Cisplatin

1,2-Dimethylhydrazine

PCNA

Colonic ACF

ABSTRACT

The use of cisplatin for the treatment of cancer is accompanied by dose-dependent adverse effects. In colorectal cancer, there is upregulation of cyclooxygenase-2 (COX-2) expression increases prostaglandin E2 (PGE2) which in turn depresses apoptosis and potentiates invasion, angiogenesis, cell-proliferation and metastasis. This study investigates a possible synergistic function for celecoxib in cisplatin-based chemotherapy against chemically-induced colon carcinogenesis in mice. Mice received fifteen injections of 1,2-dimethylhydrazine dihydrochloride (DMH; 20 mg/kg/week, s.c.) to induce colon carcinogenesis and the normal control group received equal volumes of normal saline. Mice were randomly divided into five groups, (I) normal control group, (II) DMH control group (III) DMH + cisplatin (4 mg/kg/week, i.p.) group, (IV) DMH + celecoxib (10 mg/kg/day by gavage) group and (V) DMH + cisplatin + celecoxib group. Drugs were administered starting from week eleven until the end of the experiment (week 15). Colon specimens were used to evaluate histological grades, examine intratumoral expression of Bcl2, BAX and caspase-3 and the number of proliferating nuclei. The combination of cisplatin and celecoxib was effective against malignant transformation in mice with DMH-induced colonic aberrant crypt foci (ACF). The combination group showed improvement in histological grading, the highest caspase-3 expression and the lowest Bcl2/BAX ratio and reduction by approximately 50% of immunoreactivity for proliferating cell nuclear antigen (PCNA) compared to DMH control group. Addition of celecoxib to cisplatin regimen promotes apoptosis, suppresses tumor proliferation and augments the antitumor effect of cisplatin chemotherapy in the mouse model of DMH-induced ACF.

© 2017 Production and hosting by Elsevier B.V. on behalf of Mansoura University. This is an open access article under the CC BY-NC-ND license (<http://creativecommons.org/licenses/by-nc-nd/4.0/>).

1. Introduction

Colorectal carcinoma is a major contributor to cancer burden worldwide. It is also considered as a leading cause of cancer-related mortality [1]. In Egypt, the Middle East Cancer Consortium previously reported lower rates of colorectal carcinoma (6.9/10⁵ for males and 5.1/10⁵ for females) during the period of 1999–2001 [2]. However, an increased incidence of colorectal carcinoma was observed among young patients under the age of 40. This increased trend is alarming as it is usually associated with poor prognosis [3–5].

Colorectal carcinogenesis includes changes in the colonic mucosa both at the histological and the molecular levels [6]. Mor-

phologically, aberrant crypts can be observed as a single altered crypt or as a cluster of altered crypts that form a focus termed; aberrant crypt foci (ACF). Histologically, ACF are heterogeneous group of intraepithelial lesions that exhibit variable features, ranging from almost normal or mild atypia to severe dysplasia. Indeed, ACF represent preneoplastic lesions that indicate early stages of colorectal carcinogenesis in both rodents and humans [7,8]. ACF are characterized by greater size, increased pericryptic zone and thicker epithelial lining [9]. Hence, examining the development of ACF is valuable in rodent chemoprevention studies

Cyclooxygenases have distinct expression pattern and biological activity. In colorectal carcinoma, cyclooxygenase-1 (COX-1) level remains unaltered but cyclooxygenase-2 (COX-2) expression is up-regulated [10–12]. COX-2 produces prostaglandin E2 (PGE2), which enhances the resistance to apoptosis and the potential for invasion, angiogenesis, cell-proliferation as well as metastasis [13]. Further, double knockout mice model of adenomatous poly-

* Corresponding author at: Department of Pharmacology, Faculty of Medicine, Suez Canal University, Ismailia 41522, Egypt.

E-mail address: halafathy_2@yahoo.com (H.M.F. Mohammad).

posis coli and the COX-2 genes showed lower number and reduced intestinal polyp size [14]. Furthermore, COX-2 is reported to be over-expressed in a variety of solid tumors such as prostate, colon, lung and liver cancer. Therefore, drugs that inhibit COX-2 enzyme can be promising chemo preventive agents.

Cisplatin, cis-diammine dichloroplatinum (II) $\text{Pt}(\text{NH}_3)_2(\text{Cl})_2$ is a platinum-containing chemotherapeutic drug which is used for the treatment of several types of cancers, lymphomas or germ cell tumors [15]. The chloride atoms on cisplatin are displaced by water molecules which enroll the platinum atom to preferentially bind to guanine nucleobase initiating DNA cross linking and subsequently triggering apoptosis [16]. On the other hand, celecoxib is a non-steroidal anti-inflammatory drug with higher selectivity toward inhibition of COX-2 enzyme. Steinbach et al., demonstrated that celecoxib mitigates polyps formation in patients with familial adenomatous polyposis [17]. Celecoxib exerts its anti-tumorigenic effects through inducing apoptosis in tumor cells via the activation of the anti-apoptotic kinase [18]. Interestingly, celecoxib produces antitumor effect in COX-2-deficient tumors in nude mice model and promotes apoptosis in cells not expressing COX-2 [19]. Therefore, the action of celecoxib against cancer does not solely depend on inhibiting COX-2 action.

The present study aimed to examine the chemopreventive effect of cisplatin and celecoxib combination in 1,2-dimethylhydrazine (DMH)-induced colon ACF in mice. We evaluated the expression of intratumoral caspase-3, Bcl2 and BAX to investigate the intrinsic apoptotic pathway. Furthermore, we used the proliferating cell nuclear antigen (PCNA) immunostaining to examine the impact of the combination therapy on cell proliferation.

2. Methods

2.1. Drugs and chemicals

Cisplatin (Unistin vials, 10 mg/10 ml solution) was obtained from Eimc United Pharmaceuticals (Cairo, Egypt) and was diluted with sterile saline. Celecoxib was a gift from Amoun Pharmaceutical Company (El-Obour City, Egypt). Celecoxib was suspended in 2% sodium carboxy methyl cellulose (Na-CMC; ADWIC, Cairo, Egypt) solution.

2.2. Preparation of dimethylhydrazine

1,2-Dimethylhydrazine dihydrochloride (Sigma-Aldrich®, MO, USA) was diluted with EDTA-normal saline (1 mM/L) and the pH was adjusted to 6.5 with sodium hydroxide.

2.3. Animals

Male Swiss mice (20–26 g) were purchased from the Egyptian Organization for Biological Products and Vaccines (Cairo, Egypt). Mice were maintained in a 12 h dark/light cycle at $25 \pm 3^\circ\text{C}$ and. Mice were housed in groups of six in well-ventilated clean plastic cages and all possible efforts were done to limit suffering of the mice. Cage substrate was replaced each day with food and tap water *ad libitum*. Experimental procedures were approved by the institutional research ethics committee at Faculty of Pharmacy, Suez Canal University. Date of approval: June 2014.

2.4. Experimental design

After a 1-week acclimatization period, sixty male mice were randomly divided to five experimental groups; each group consisted of 12 animals. Group 1 (Normal control group) in which the mice received normal saline (20 ml/kg/week, sc). Group 2

(DMH control group): Mice injected with DMH (20 mg/kg; sc) weekly for a total of 15 injections [20]. Group 3 (DMH + cisplatin): mice received weekly injections of DMH and given cisplatin (4 mg/kg/week, i.p.) during the last 5 weeks of the experiment. Group 4 (DMH + celecoxib group): mice received weekly injections of DMH and administered celecoxib (10 mg/kg/day) by gavage during the last 5 weeks of the experiment. Group 5 (DMH + cisplatin + celecoxib group): mice received weekly injections of DMH and received cisplatin (4 mg/kg/week, i.p.) plus celecoxib (10 mg/kg/day) [drugs were given from week 11 to week 15]. Mice were monitored in a daily manner to detect any type of discomfort and to register the number of surviving mice.

2.5. Tissue processing

At the end of week 15, mice were anesthetized with ether and sacrificed by cervical dislocation. Then, mice were autopsied and the colon was excised, opened along the horizontal axis and flushed using ice-cold saline. Next, colon sections were flattened and fixed in 10% phosphate buffered formalin for 1 day. Tissue samples were processed, embedded in paraffin wax, cut into sections (4- μm) and finally stained with hematoxylin and eosin (H&E) for histological diagnosis of tumors [21].

2.6. Histopathological examination of colon specimens

Colon sections were examined under a light microscope (Olympus CX21, Japan). A low power ($\times 10$ magnification) was used to visualize the whole tissue sections while scoring was performed using a high power ($\times 40$ magnification). Morphometric scoring was employed using image analyzer. A grading system was established for the degree of cell dysplasia. In which dysplasia was considered as aberrant structure, hyperplasia was considered upon observing increasing size and number of cells, mucosal inflammation was considered when inflammatory cell infiltration, focal inflammatory cell aggregation, lymphoid proliferation, congested blood vessels and fibrosis were detected. Score 0 was assigned for normal sections that appear free from any signs of dysplasia, hyperplasia or inflammation. Score 1 was assigned when no dysplasia but mild inflammatory reaction was observed. Score 2 was assigned for moderate inflammatory reaction with or without dysplasia. Score 3 was assigned for dysplasia/or hyperplasia with severe inflammation. Score 4 was assigned in cases of severe inflammatory reaction with dysplastic or hyperplastic activity and fibrosis [22].

2.7. Immunohistochemical staining

Immunohistochemical staining was performed employing a 3-step indirect technique based on the labelled avidin-biotin peroxidase complex (ABC) method. Colon sections were deparaffinized, rehydrated and boiled with 0.01 M citrate buffer, pH = 6.0, for 15 min for antigen retrieval. Next, tissue specimens were maintained at room temperature and covered for 1 h in 1% bovine serum albumin. This was followed by an overnight incubation (at 4°C) with the different primary antibodies. On the next day, biotinylated secondary antibodies were added to the tissue sections. Then, the avidin-biotin-peroxidase complex was added (LAB-SA detection system; Invitrogen) Visualization of the reaction was performed using a 0.05% solution of 3,3-diaminobenzidine which produces a dark brown precipitate. Tissue sections were subjected to counterstaining with Mayer's hematoxylin, and dehydrated in ascending alcohol series. Then, sections were cleared in xylene and finally mounted with DPX. Sections for the negative control were incubated without the primary antibodies. In this study, rabbit polyclonal antibodies against caspase-3 (1:100), mouse monoclonal antibodies against Bcl2 and BAX (1:100,

Thermo Fischer Scientific, Fremont, CA, USA) and mouse monoclonal antibodies against PCNA (1:100, Abcam, Cambridge, UK) were utilized. After completing the staining process, slides were investigated by the aid of a light microscope (Olympus CX21, Japan).

2.8. Morphometric analysis

Image analysis was performed using image analyzer (Super eye-Heidi Software Co., Cairo, Egypt). Three parameters were measured: the histological scores, the optical density of caspase-3, Bcl2 and BAX immunoreactivity and the number of PCNA immunopositive nuclei. The measurements were recorded in photomicrographs of ten non-overlapping fields from ten different sections of five different mice in each group at $\times 400$ magnification.

2.9. Statistical analysis

Data from each experiment were tabulated and represented as mean \pm SEM. Parameters with Gaussian distribution were compared using one-way ANOVA analysis followed by Bonferroni's test for multiple-comparisons. Histological scores were analyzed by the Kruskal–Wallis test followed by Dunnett's test for comparisons between groups. Data were analyzed using SPSS program version 22 (Chicago, IL, USA). The percent of surviving mice in each group was analyzed using Chi-square test. Data were two-tailed and the level of significance was set at $P < 0.05$.

3. Results

3.1. Percent mortality

Mortality percentage was recorded in the different groups. In the DMH control group, we observed a 25% mortality (3 out of 12 mice), whereas, cisplatin and celecoxib groups showed similar mortality percentages (34%; 4 out of 12). The mortality of mice in the combination group (DMH + cisplatin + celecoxib) was 41.7% (5 out of 12), but it was not significantly different from the DMH control group (Fig. 1).

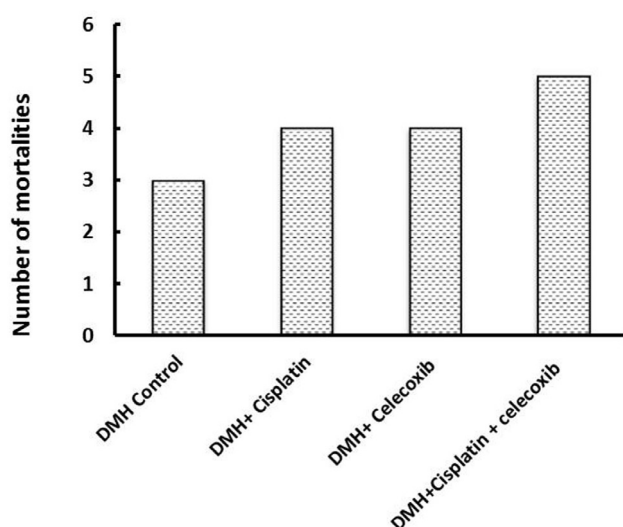


Fig. 1. Effect of cisplatin and celecoxib on mice mortality in 1,2-dimethylhydrazine (DMH)-induced Aberrant Crypt Foci (ACF). There was no statistical difference in the mortality percentage among the different groups, $n = 12$ at the beginning of the experiment.

3.2. Histological examination and tumor grading

On one hand, gross examination of colon did not reveal any lesions or carcinogenic masses. On the other hand, the light microscopic examination of H&E stained colon sections revealed normal colon mucosa in normal control group; consisted of straight, simple tubular glands (crypts of Lieberkühn) that extend through the full thickness of the mucosa. These crypts were lined by surface absorptive cells and vacuolated goblet cells. Submucosa (loose connective tissue), musculosa (smooth muscle fibers) and serosa were also identified. In the DMH control group, the colon mucosa showed multiple crowded packed crypts of different lengths. The epithelial cells lining the crypts were proliferating and increased in size (signs of hyperplasia). Concurrently most of their nuclei were large in size and hyperchromatic (signs of dysplasia). Moreover, these crypts having numerous focal areas of cell proliferation (ACF) and severe aggregation of inflammatory cells in the lamina propria of mucosa. On the other hand, colon mucosa in DMH + cisplatin group had straight crypts that were less packed than those in DMH control. These crypts were lined by cells, with nuclei that were less in hyperchromasia and size, in comparison with those of DMH control. Further, focal areas of cell proliferation in crypts and mild aggregations of infiltrating inflammatory cells were observed. The colon mucosa in DMH + celecoxib group had crypts of different lengths and was more packed than those in DMH + cisplatin group but less than those of the DMH control group. These crypts were lined by cells that contain larger and hyperchromatic nuclei than those of DMH + cisplatin group but still less than those in DMH control group. Moreover, some focal areas of cell proliferation were more abundant as compared to those observed in DMH + cisplatin group, but less than those in DMH control group. Lastly, examination of colon mucosa in DMH + cisplatin + celecoxib group revealed that their crypts were smaller in size and reduced in packing. These crypts had less number of hyperchromatic nuclei and fewer focal areas of cell proliferation compared to the other groups (Fig. 2A).

Statistical analysis of the median histologic scores and their quartiles in the experimental groups highlighted significant differences between DMH + cisplatin group, DMH + celecoxib group or DMH + cisplatin + celecoxib group in comparison with DMH control group ($P < 0.05$). Data analysis using the Kruskal–Wallis test followed by Dunnett's test demonstrated significant difference between the combination of DMH + cisplatin + celecoxib in comparison to DMH control and DMH + celecoxib (Fig. 2B).

3.3. Caspase-3 immunostaining

Light microscopic examination of the immunohistochemical stained colon sections for caspase-3 revealed that the cytoplasm of epithelial cells lining crypts as well as that of some cells of lamina propria of the DMH control, DMH + cisplatin, DMH + celecoxib and DMH + cisplatin + celecoxib groups were positively stained with different intensities (Fig. 3A). Statistical analysis of the mean optical density of their immunoreactivity revealed that DMH + cisplatin group showed approximately 1.9-fold increase in caspase-3 immunostaining compared to DMH control group. However, DMH + celecoxib group showed about 1.4-fold increase in colon expression of caspase-3 compared to DMH control group. In addition, DMH + celecoxib group showed lower staining for caspase-3 in comparison to the DMH + cisplatin group ($P < 0.05$, Fig. 3B). Further, DMH + cisplatin + celecoxib group showed a 2-fold increase in caspase-3 expression compared to DMH control group and this value was not different from that caused by cisplatin monotherapy (Fig. 3B).

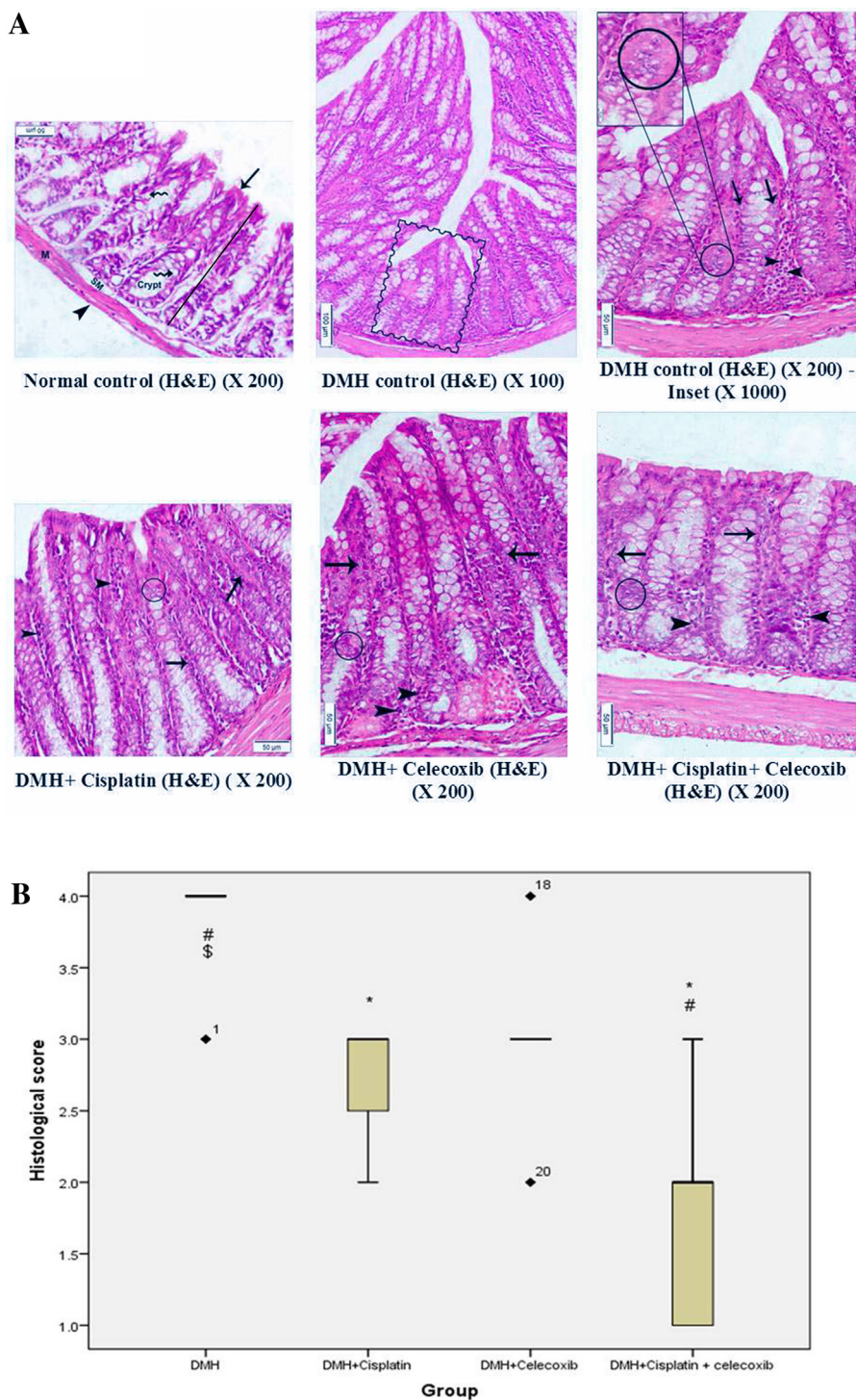
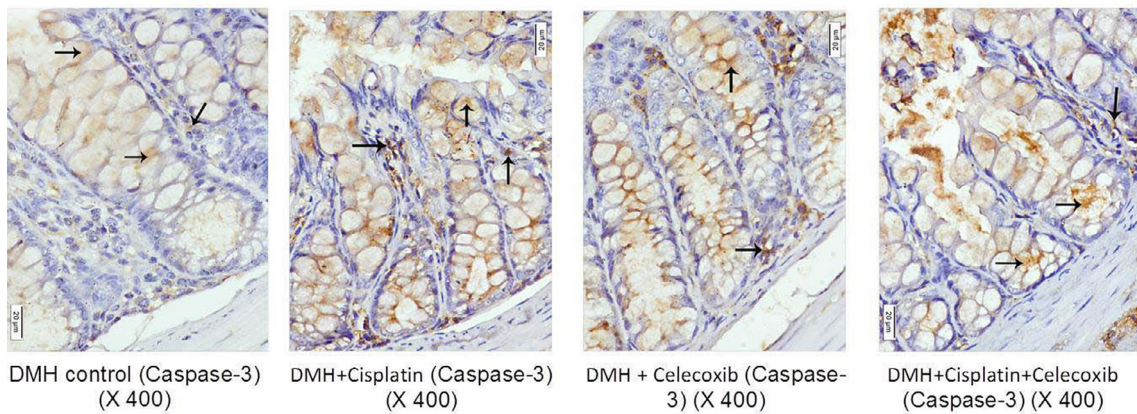


Fig. 2. Effect of cisplatin and celecoxib on the histopathological picture of colon in colon tissues of mice in DMH-induced ACF. A). Photomicrographs showing colon sections from mice, stained with hematoxylin and eosin in the different experimental groups. A photomicrograph of a colon section in normal control group showing the mucosal thickness (bar), the crypts which are lined by surface absorptive cells (arrow) and goblet cells (wavy arrows), submucosa (SM), musculosa (M), and serosa (arrowhead) appeared. The crypts are straight, simple tubular glands that extend through the full thickness of the mucosa. A photomicrograph of a colon section in DMH control group, showing multiple crypts of different lengths (Rectangle) are crowded. A photomicrograph of a colon section in DMH control group, showing epithelial cells line the crypts have large, hyperchromatic nuclei (arrows), a focal area of cell proliferation (small circle), and severe aggregation of inflammatory cells (arrowheads). The inset in the upper left corner of this photomicrograph has the magnification of the closely packed proliferated cells (large circle). A photomicrograph of a colon section in DMH + cisplatin group showing straight crypts of different lengths and some of these crypts are lined by cells that have moderate chromasia (arrows). Mild infiltration of inflammatory cells (arrowheads) and a focal area of cell proliferation (circle) were present. A photomicrograph of a colon section in DMH + celecoxib group, showing relatively straight crypts which are lined by cells with hyperchromatic nuclei (arrows) are observed. Further, mild inflammatory cells (arrowheads) infiltrates and a focal area of cell proliferation (circle) were appearing. A photomicrograph of a colon section in DMH + cisplatin + celecoxib group, showing straight crypts lined by more or less normal cells with small and less hyperchromatic nuclei (arrows). Minimal inflammatory cells (arrowheads) infiltrates and a focal area of cell proliferation (circle) were seen. B) A box plot chart for the median histologic score and quartiles in the experimental groups. 1,2-Dimethylhydrazine (DMH, 20 mg/kg/week, s.c.) was used to induce ACF in mice. Data were analyzed using the Kruskal–Wallis test followed by Dunnett's test at $P < 0.05$. * Compared to DMH control, # Compared to (DMH + cisplatin), \$ Compared to (DMH + celecoxib). Data were analyzed using SPSS program version 22.

A



B

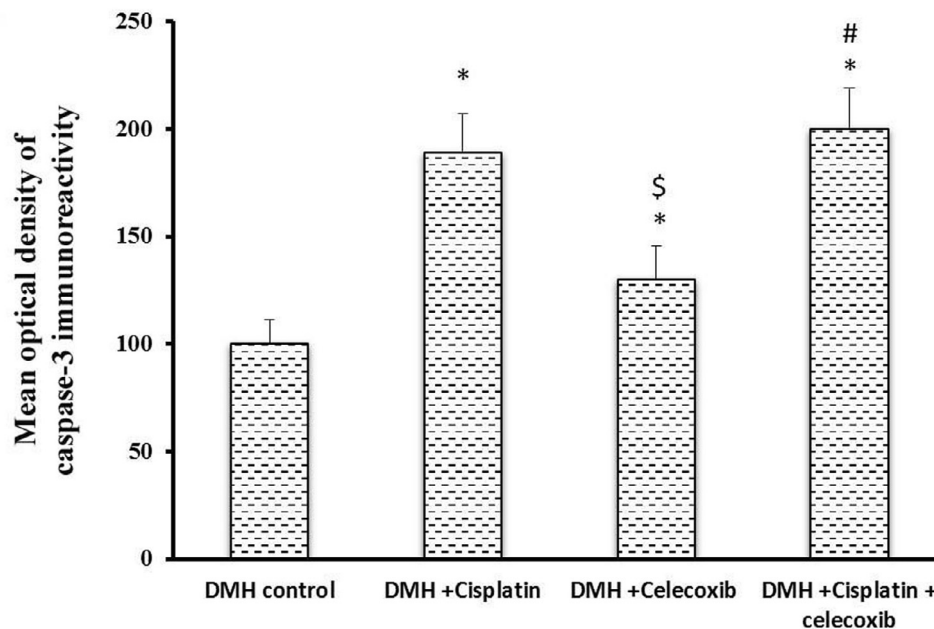


Fig. 3. Effect of cisplatin and celecoxib on the expression of caspase-3 in colon tissues of mice in DMH-induced ACF. A) Photomicrographs showing immunohistochemical staining for caspase-3 in the colon sections in experimental groups. Photomicrographs of colon sections of DMH control, DMH + cisplatin, DMH + celecoxib and DMH + cisplatin + celecoxib groups showing, cytoplasm of epithelial cells lining the crypts as well as that of some cells in the lamina propria stained brown due to their contents of caspase-3 (arrows). B) A column chart demonstrating the mean optical density of caspase-3 immunoreactivity in the experimental groups. Data were presented as mean \pm SEM and analyzed using one-way ANOVA followed by Bonferroni's post hoc test at $P < 0.05$. *Compared to DMH control, \$Compared to DMH + cisplatin, #Compared to DMH + celecoxib.

3.4. Bcl2 and BAX immunohistochemical staining and calculation of the Bcl2/BAX ratio

Light microscopic examination of the immunohistochemical stained colon sections for Bcl2 and BAX (Figs. 4 and 5A, respectively) revealed that the cytoplasm of epithelial cells lining crypts and some cells in the lamina propria in DMH control group and groups treated with DMH + cisplatin, DMH + celecoxib or DMH + cisplatin + celecoxib were positively stained with different intensities. Statistical analysis of the mean optical density of their immunoreactivity indicated that monotherapy with cisplatin or celecoxib as well as the combination therapy had reduced Bcl2 expression in comparison with DMH control group (Fig. 4B). Moreover, the pro-apoptotic protein, BAX, was up-regulated in colon of celecoxib group and the combination group when compared to

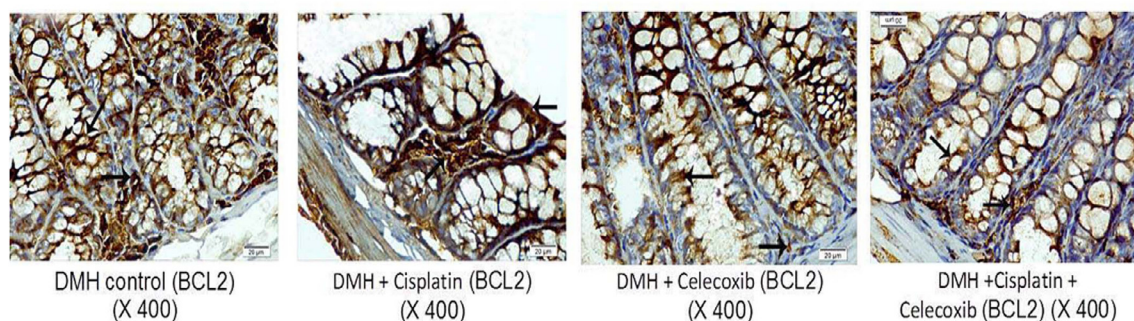
DMH control group (Fig. 5B) suggesting that celecoxib followed this intrinsic pathway of apoptosis shifting the equilibrium from survival to apoptosis.

Calculating the Bcl2/BAX ratio highlighted significant decreases in all drug treated groups compared to DMH control group. Bcl2/BAX ratio in DMH + celecoxib group was lower than that obtained in DMH + cisplatin group. Moreover, combination of cisplatin plus celecoxib produced lower Bcl2/BAX ratio compared to their respective monotherapies (Fig. 5C).

3.5. Determination of colon expression for the proliferation cell nuclear antigen

Light microscopic examination of the immunohistochemical stained colon sections for PCNA revealed that nuclei of some

A



B

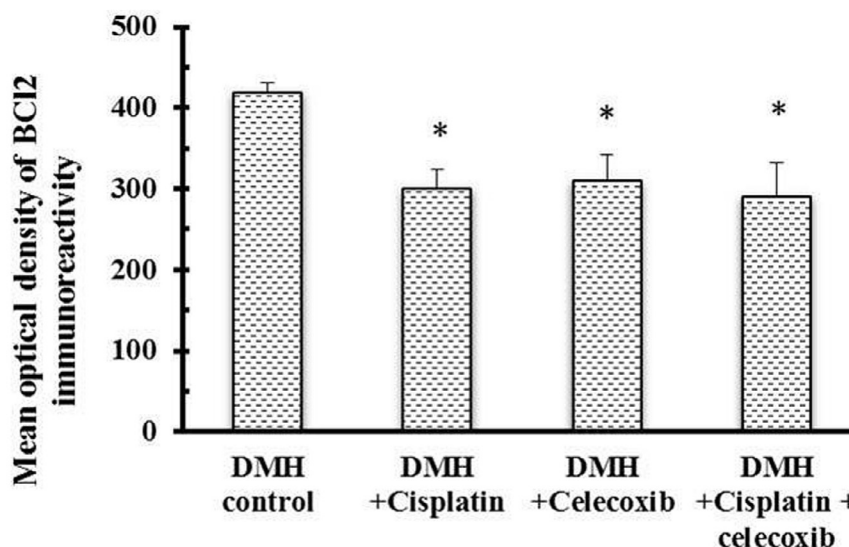


Fig. 4. Effect of cisplatin and celecoxib on expression of Bcl2 in colon tissues of mice in DMH-induced ACF. A) Photomicrographs showing the immunohistochemical staining for Bcl2 in the colon sections of different experimental groups. These photomicrographs of colon sections in DMH control, DMH + cisplatin, DMH + celecoxib, and DMH + cisplatin + celecoxib groups showing the cytoplasm of epithelial cells lining the crypts and some cells in the lamina propria stained brown indicating their contents of Bcl2 (arrows). B) A column chart demonstrating the mean optical density of Bcl2 immunoreactivity in the experimental groups. Data were presented as mean \pm SEM and analyzed using one-way ANOVA followed by Bonferroni's post hoc test at $P < 0.05$. *Compared to DMH control, [§]Compared to DMH + cisplatin, [§]Compared to DMH + celecoxib.

epithelial cells that lining crypts in addition to some cells in lamina propria of DMH control group and groups treated with cisplatin and/or celecoxib were stained brown indicating the presence of PCNA (Fig. 6A). Consequently, this indicates the proliferating power of the epithelial cells and the cells in the lamina propria. Monotherapy with cisplatin or celecoxib decreased the number of PCNA positive nuclei (20%) in comparison with DMH control group. In addition, the combination of cisplatin plus celecoxib induced the maximum suppressive effect on the number of PCNA positive nuclei (50%) compared with DMH control group ($P < 0.05$, Fig. 6B).

4. Discussion

In cancer treatment, the use of combination therapies is preferred over monotherapy owing to the fact that combination therapies offer a reduction in dose and toxicity and decrease the likelihood of developing acquired drug resistance [23]. In the current *in vivo* study, the chemopreventive effect of celecoxib either alone or in combination with cisplatin against DMH-induced ACF in mice was investigated. The administration of DMH caused DNA methylation resulting in ACF formation in mice colons [8,22,24]. Simi-

larly, the greatest number of PCNA positive cells was observed in the DMH control group.

ACF were identified in mucosal layer of patients at high risk of developing colorectal carcinoma [25] and rodents receiving carcinogenic agents [9]. Therefore, ACF is commonly used in assessing the protective role of natural or pharmacological agents in the development of colon carcinogenesis [26]. Histological features of ACF were detected in milder forms as mild atypia and severe forms as severe dysplasia. Dysplasia is considered as a predisposing factor for an organ to carcinogenesis [27]. Therefore, ACF are considered as useful markers for screening drugs or new compounds for their chemopreventive activities [26,28]. The administration of either cisplatin or celecoxib alone decreased the ACF formation and enhanced the histological score of the colonic mucosa compared to the DMH control group. The combination treatment celecoxib (10 mg/kg) plus cisplatin proved to be the most successful. ACF were significantly smaller and their histological grading was significantly better than the corresponding monotherapy without significantly affecting the mortality percentage.

Apoptosis is a crucial process in maintaining cellular homeostasis. Sensitivity of a normal or cancer cell to apoptosis is dependent on the balance between the pro-apoptotic and anti-apoptotic genes. BAX gene is a member of Bcl2 family that regulates apoptotic cell

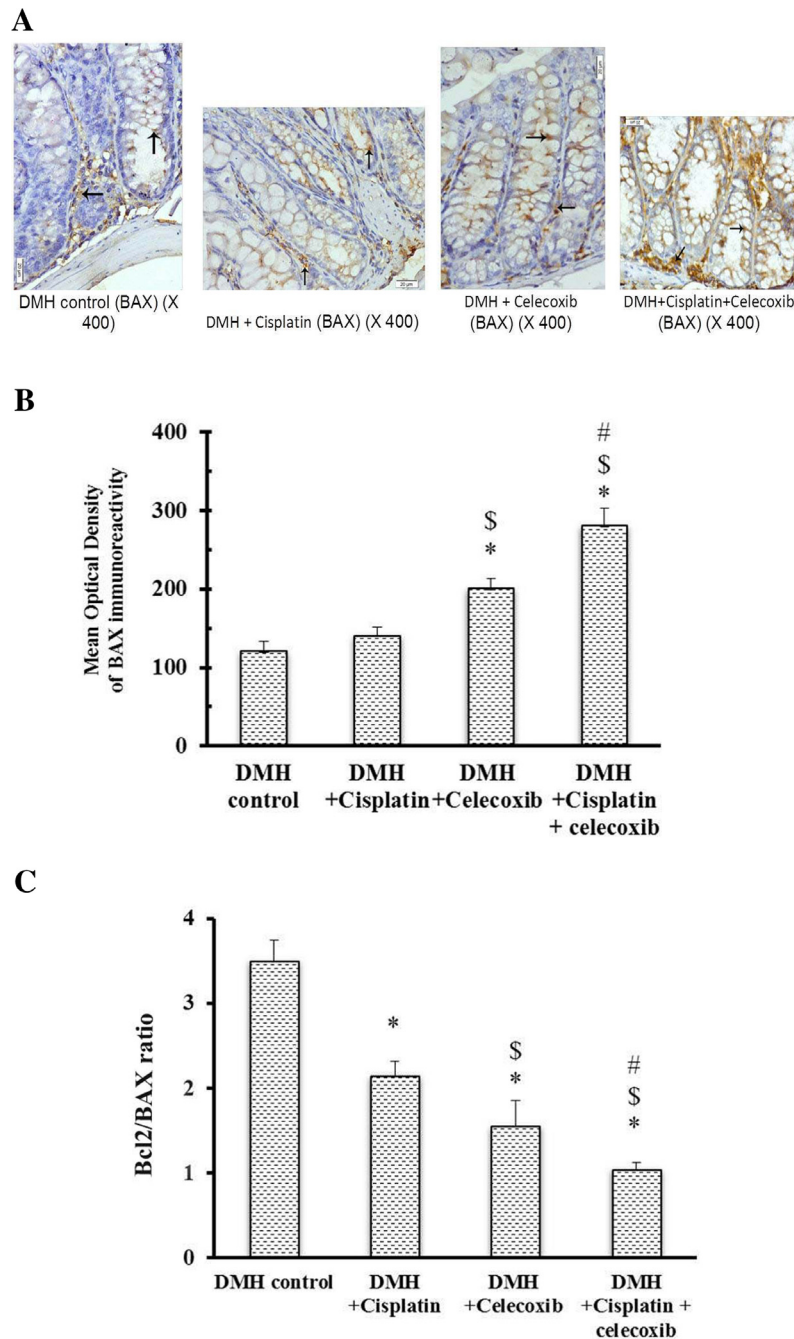


Fig. 5. Effect of cisplatin and celecoxib on expression of BAX in colon tissues of mice in DMH-induced ACF. A) Photomicrographs showing the immunohistochemical staining for BAX in the colon sections from different experimental groups. These photomicrographs of colon sections in DMH control, DMH + cisplatin, DMH + celecoxib, and DMH + cisplatin + celecoxib groups showing the cytoplasm of epithelial cells lining the crypts and some cells in the lamina propria stained brown due to their contents of BAX (arrows). B) A column chart demonstrating the mean optical density of BAX immunoreactivity in the experimental groups. Data were presented as mean \pm SEM and analyzed using one-way ANOVA followed by Bonferroni's post hoc test at $P < 0.05$. * Compared to DMH control, \$ Compared to DMH + cisplatin, # Compared to DMH + celecoxib. C) A Column chart demonstrating the mean optical density for Bcl2/BAX ratio in the experimental groups. Data were presented as mean \pm SEM and analyzed using one-way ANOVA followed by Bonferroni's post hoc test at $P < 0.05$. * Compared to DMH control, \$ Compared to DMH + cisplatin, # Compared to DMH + celecoxib.

death. The Bcl2 family consists of 14 types of pro-apoptotic or anti-apoptotic proteins. On the other hand, Bcl2 gene inhibits apoptosis and extends the cell survival. The ratio of Bcl2 to BAX determines the susceptibility of a cell to apoptosis [29]. Caspase enzymes are cysteine proteases that have responsibility for initiating and executing phases of apoptotic cell death. Several reports indicated that up-regulation of mRNA for caspase-3 positively correlates with cell apoptosis [30–32]. Therefore, in this study, we evaluated the apoptosis process via studying the Bcl2 (apoptosis inhibitor) to BAX

(apoptosis promoter) ratio along with caspase-3 expression in various treatment regimens. ACF in the treatment groups showed a higher rate of apoptosis as verified by increment in caspase-3 expression and the decreased Bcl2/BAX ratio. Monotherapy with celecoxib increased BAX expression and slightly diminished Bcl2 expression. The pro-apoptotic effect of celecoxib came in accordance with an *in vitro* study on HT29 cells, where celecoxib treatment induced BAX and down-regulated Bcl2 expression [33–36]. Similarly, an *in vivo* model of colorectal carcinoma in nude

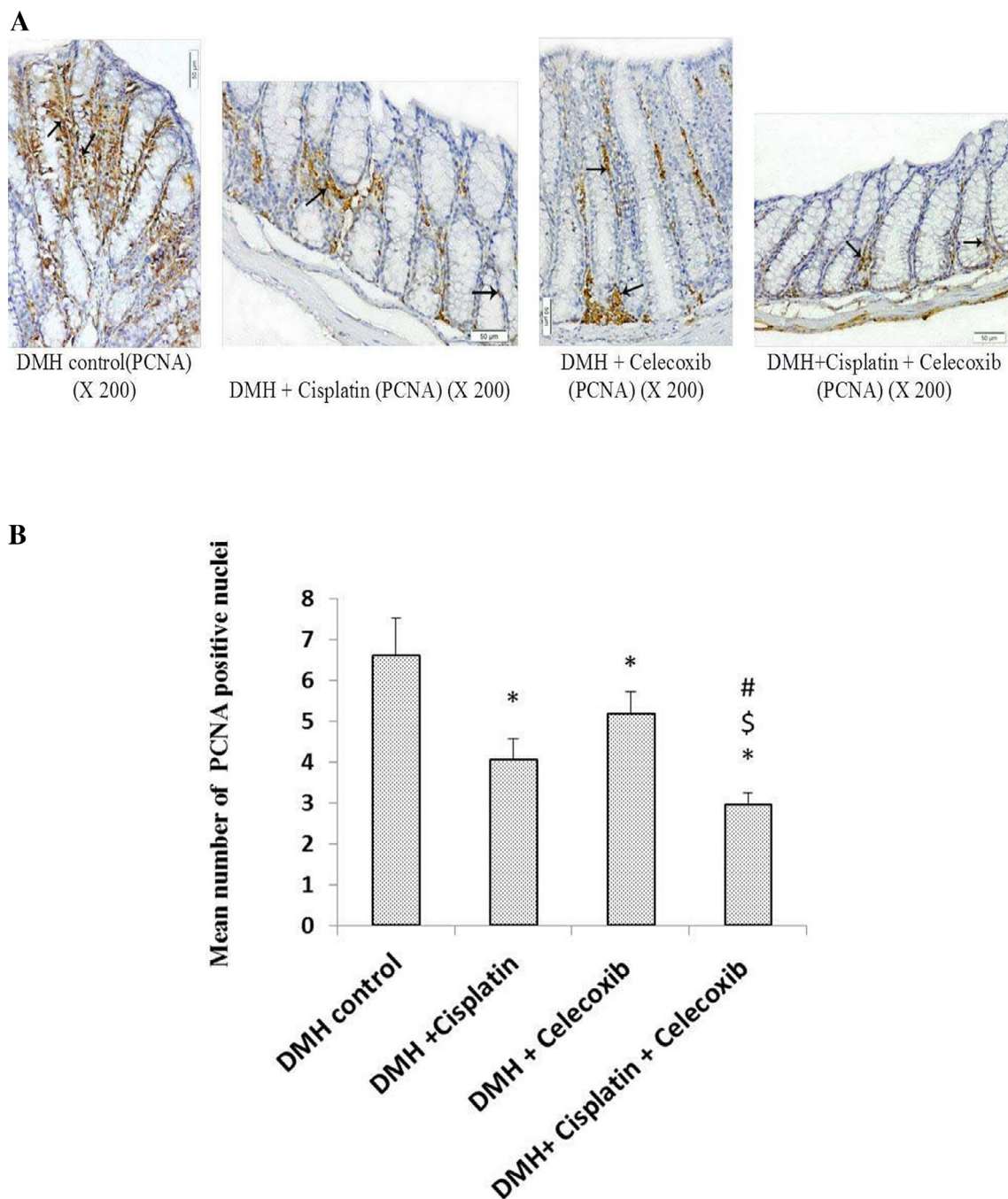


Fig. 6. Effect of cisplatin and celecoxib on number of PCNA immunopositive nuclei in colon tissues of mice in DMH-induced ACF. A) Photomicrographs showing the immunohistochemical staining for PCNA in the colon sections from different experimental groups. Photomicrographs of colon sections in DMH control, DMH + cisplatin, DMH + celecoxib and DMH + cisplatin + celecoxib groups showing brown stained nuclei (arrows) of epithelial cells lining the crypts and those in the lamina propria demonstrating the presence of PCNA. B) A column chart demonstrating mean number of PCNA immunopositive nuclei in experimental groups. Data were presented as mean \pm SEM and analyzed using one-way ANOVA followed by Bonferroni's post hoc test at $P < 0.05$. *Compared to DMH control, $^{\$}$ Compared to DMH + cisplatin, $^{\#}$ Compared to DMH + celecoxib.

mice showed that celecoxib resulted in upregulated caspase-3 [30,37]. However, to the best of our knowledge, this is the first study that examines the effect of celecoxib on Bcl2, BAX and caspase-3 mediated apoptotic pathways in DMH-induced colon carcinogenesis in mice. On the other hand, cisplatin treatment slightly suppressed Bcl2 without affecting BAX expression. The combination treatment produced the maximal pro-apoptotic effect as it showed the highest caspase-3 expression and the lowest Bcl2/BAX ratio.

Balance between apoptosis and cell proliferation regulate colorectal carcinogenesis [38,39]. In our study, immunohistochemical analysis revealed that PCNA was overexpressed in the untreated DMH control group. Treatment with either cisplatin or celecoxib showed around 20% reduction in PCNA immunoreactivity, whereas, PCNA immunoreactivity was reduced by around 50% in the combination treatment group. Therefore, indicating the synergistic effect of celecoxib and cisplatin combination in cancer treatment.

Indeed, this study showed that celecoxib promotes apoptosis, suppresses tumor proliferation and consequently, potentiates the antitumor effect of cisplatin when used in combination in a DMH-induced ACF model.

5. Conclusion

This study indicated that celecoxib inhibits tumor growth and augments the antitumor effect of cisplatin in DMH-induced ACF in mice. This effect is at least in part mediated by induction of apoptosis and suppression of cell proliferation. Hence, celecoxib is a promising add-on drug with cisplatin for colon cancer treatment.

Funding source

Authors received no fund from any organization or company.

Ethics

All applicable international, national, and/or institutional guidelines for the care and use of animals were followed.

Acknowledgments

The Authors thank Dr. Mohamed Kamal, Department of Pathology at School of Medicine in Suez Canal University, for providing help in capturing some of photographs. Authors are grateful to Dr. Abdel-Salam G. Abdel-Salam, department of statistics, Faculty of Economics and Political Sciences, Cairo University for his advice in statistical analysis. Thanks for Amoun Pharmaceutical Company (Cairo, Egypt) for kindly providing celecoxib.

References

- [1] Ferlay J, Shin HR, Bra F, et al. Estimates of worldwide burden of cancer in 2008: GLOBOCAN. *Int J Cancer* 2010;127:2893–917.
- [2] Freedman LS, Edwards BK, Ries LAG, Young JL, editors. National Cancer Institute (US), Middle East Cancer Consortium. Cancer Incidence in Four Member Countries (Cyprus, Egypt, Israel, and Jordan) of the Middle East Cancer Consortium (MECC) Compared with US SEER. Bethesda, MD: National Cancer Institute, 2006.
- [3] Nieminen TT, Shoman S, Eissa S, Peltomäki P, Abdel-Rahman WM. Distinct genetic and epigenetic signatures of colorectal cancers according to ethnic origin. *Cancer Epidemiol Biomarkers Prev* 2012;21:202–11.
- [4] Veruttipong D, Soliman A, Gilbert S, et al. Age distribution, polyps, and rectal cancer in the Egyptian population-based cancer registry. *World J Gastroenterol* 2012;18:3997–4003.
- [5] Gado A, Ebeid B, Abdelmohsen A, Axon A. Colorectal cancer in Egypt is commoner in young people: Is this cause for alarm? *Alex J Med* 2014;50:197–201.
- [6] Jass JR. Pathogenesis of Colorectal Cancer. *Surg Clin North Am* 2002;82:891–904.
- [7] Cheng L, Lai MD. Aberrant crypt foci as microscopic precursors of colorectal cancer. *World J Gastroenterol* 2003;9:2642–9.
- [8] Suzui M, Morioka T, Yoshimi N. Colon preneoplastic lesions in animal models. *J Toxicol Pathol* 2013;26:335–41.
- [9] Bird RP. Role of aberrant crypt foci in understanding the pathogenesis of colon cancer. *Cancer Lett* 1995;93:55–71.
- [10] Dubois RN, Abramson SB, Crofford L, et al. Cyclooxygenase in biology and disease. *FASEB J* 1998;12:1063–73.
- [11] Gupta RA, DuBois RN. Colorectal cancer prevention and treatment by inhibition of cyclooxygenase-2. *Nat Rev Cancer* 2011;11:21.
- [12] Marnett LJ, DuBois RN. COX-2: a target for colon cancer prevention. *Annu Rev Pharmacol Toxicol* 2002;42:55–80.
- [13] Kawai N, Tsujii M, Tsuji S. Cyclooxygenases and colon cancer. *Prostaglandins Other Lipid Mediat* 2002;68–69:187–96.
- [14] Oshima M, Dinchuk JE, Kargman SL, et al. Suppression of intestinal polyposis in *Apc^{Δ716}* knockout mice by inhibition of cyclooxygenase 2 (COX-2). *Cell* 1996;87:803–9.
- [15] Grosch S, Tegeder I, Niederberger E, Brautigam L, Geisslinger G. OX-2 independent induction of cell cycle arrest and apoptosis in colon cancer cells by the selective COX-2 inhibitor celecoxib. *FASEB J* 2001;15:2742–4.
- [16] Alderden RA, Hall MD, Hambley TW. The discovery and development of celecoxib. *J Chem Educ* 2006;83:728–34.
- [17] Steinbach G, Lynch PM, Phillips RK, Wallace MH, Hawk E, et al. The effect of celecoxib, a cyclooxygenase-2 inhibitor, in familial adenomatous polyposis. *N Engl J Med* 2000;342:1946–52.
- [18] Hsu AL, Ching TT, Wang DS, Song X, Rangnekar VM, Chen CS. The cyclooxygenase-2 inhibitor celecoxib induces apoptosis by blocking Akt activation in human prostate cancer cells independently of Bcl-2. *J Biol Chem* 2000;275:11397–403.
- [19] Ishida S, Lee J, Thiele DJ, Herskowitz I. Uptake of the anticancer drug cisplatin mediated by the copper transporter Ctr1 in yeast and mammals. *Proc Natl Acad Sci USA* 2002;99:14298–302.
- [20] Colussi C, Fiumicino S, Giuliani A, et al. 1,2-Dimethylhydrazine-induced colon carcinoma and Lymphoma in *msh2^{-/-}* mice. *JNCI* 2001;93:1534–40.
- [21] Bancroft JD, Stevens A. Theory and practice of histological techniques. 4th Ed. New York and London: Churchill Livingstone; 1996 (pp. 145–146).
- [22] Zaafar DK, Zaitone SA, Moustafa YM. Role of metformin in suppressing 1,2-dimethylhydrazine-induced colon cancer in diabetic and non-diabetic mice: effect on tumor angiogenesis and cell proliferation. *PLoS ONE* 2014;9:e100562.
- [23] Gaikwad A, Prchal JT. Study of two tyrosine kinase inhibitors on growth and signal transduction in polycythemia vera. *Exp Hematol* 2007;35:1647–56.
- [24] Jackson PE, Cooper DP, O'Connor PJ, Povey AC. The relationship between 1,2-dimethylhydrazine dose and the induction of colon tumours: tumour development in female SWR mice does not require a K-ras mutational event. *Carcinogenesis* 1999;20:509–13.
- [25] Pretlow TP, Barrow BJ, Ashton WS, et al. Aberrant crypts: putative preneoplastic foci in human colonic mucosa. *Cancer Res* 1991;51:1564–7.
- [26] Wargovich MJ, Jimenez A, McKee K, et al. Efficacy of potential chemopreventive agents on rat colon aberrant crypt formation and progression. *Carcinogenesis* 2000;21:1149–55.
- [27] Boivin GP, Washington K, Yang K, et al. Pathology of mouse models of intestinal cancer: consensus report and recommendations. *Gastroenterology* 2003;124:762–77.
- [28] Raju J. Azoxymethane-induced rat aberrant crypt foci: relevance in studying chemoprevention of colon cancer. *World J Gastroenterol* 2008;14:6632–5.
- [29] Yang B, Johnson TS, Thomas GL, et al. A shift in the Bax/Bcl-2 balance may activate caspase-3 and modulate apoptosis in experimental glomerulonephritis. *Kidney Int* 2002;62:1301–13.
- [30] Carrillo C, Cavia Mdel M, Alonso-Torre SR. Antitumor effect of oleic acid; mechanism of action: a review. *Nutr Hosp* 2012;27:1860–5.
- [31] Zhang DQ, Guo Q, Zhu JH, Chen WC. Increase of cyclooxygenase-2 inhibition with celecoxib combined with 5-FU enhances tumor cell apoptosis and antitumor efficacy in a subcutaneous implantation tumor model of human colon cancer. *World J Surg Oncol* 2013;11:6.
- [32] Amptoulach S, Lazaris AC, Giannopoulou I, et al. Expression of caspase-3 predicts prognosis in advanced noncardia gastric cancer. *Med Oncol* 2015;32:416.
- [33] Gallicchio M, Rosa AC, Dianzani C, Brucato L, Collino M, Fantozzi R. Celecoxib decreases expression of the adhesion molecules ICAM-1 and VCAM-1 in a colon cancer cell line (HT29). *Br J Pharmacol* 2008;153:870–8.
- [34] Chen Y, Tsai Y, Tseng S. Combined valproic acid and celecoxib treatment induced synergistic cytotoxicity and apoptosis in neuroblastoma cells. *Anticancer Res* 2011;31:2231–40.
- [35] Jeon Y, Suh YJ. Synergistic apoptotic effect of celecoxib and luteolin on breast cancer cells. *Oncol Rep* 2013;29:819–25.
- [36] Jendrosseck V. Targeting pathways of celecoxib in cancer. *Cancer Lett* 2013;332:313–24.
- [37] Rosas C, Sinning M, Ferreira A, et al. Celecoxib decreases growth and angiogenesis and promotes apoptosis in a tumor cell line resistant to chemotherapy. *Biol Res* 2014;47:27.
- [38] Sinicrope FA, Roddey G, McDonnell TJ, Shen Y, Cleary KR, Stephens LC. Increased apoptosis accompanies neoplastic development in the human colorectum. *Clin Cancer Res* 1996;2:1999–2006.
- [39] Lin MX, Wen ZF, Feng ZY, He D. Expression and significance of Bmi-1 and Ki67 in colorectal carcinoma tissues. *Chin J Cancer* 2008;27:568–73.